ANISOTROPY EFFECTS ON LAMB WAVES IN COMPOSITE PLATES

R. L. Bratton and S. K. Datta

Department of Mechanical Engineering and CIRES
University of Colorado
Boulder, CO 80309-0427

A. H. Shah

Department of Civil Engineering
University of Manitoba
Winnipeg, Canada R3T 2N2

INTRODUCTION

There is currently considerable interest in metal matrix composites for applications in space structures. Both particle and fiber reinforced materials are under investigation. Our recent studies [1,2] have shown that these materials can usually be characterized as transversely isotropic having five distinct elastic stiffnesses. Using a wave scattering formalism, models of their rheology were derived for predicting these five elastic stiffnesses. Manufactured parts (plates, tubes, etc.) containing these materials have unique properties, which are subjects of considerable interest for ultrasonic nondestructive evaluations, impact response, and vibrations. In this paper we have studied guided wave propagation in plates of two different materials: SiC particle-reinforced aluminum alloy and graphite fiber-reinforced magnesium. As was shown in previous investigations [1,2], both of these materials show transverse isotropic symmetry. Here it has been assumed that the axis of symmetry lies in the plane of the plate. Thus for propagation in an arbitrary direction parallel to the plate, the motion is three dimensional, i.e., the equations governing the three components of displacement are coupled. This causes considerable complexity in the dispersion equation. Here we have presented solutions to this equation showing different behaviors for the two materials.

Wave propagation in homogeneous isotropic plates and monoclinic plates have been studied extensively using exact and approximate methods by Mindlin and co-workers [3-6]. Recently, harmonic wave propagation in fiber-reinforced composites has been the focus of investigations using both numerical and analytical technqiues. Representative of the numerical methods is the stiffness method discussed in [7-10]. Analytical models for leaky Lamb waves in a fluid coupled composite plate have been presented in [11-12]. In the following section we derive the dispersion equation by solving analytically the differential equations governing the displacement components and satisfying the boundary conditions for a free-free plate.

GOVERNING EQUATIONS

Time harmonic waves of the form shown in Eq. (1) below are considered to represent the elastic wave guided by the plate, where ω represents the circular frequency (rad/sec), K is the wavenumber (inverse of the wave length) in the direction of propagation, $\underset{\sim}{u}(z)$ is the displacement, and $\underset{\sim}{f}(z)$ is an undertermined function of z

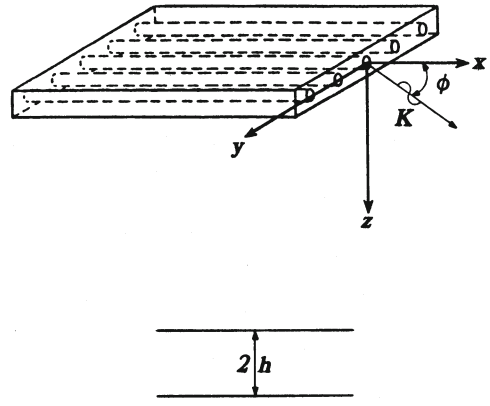

Fig. 1. Uniaxial fiber reinforced plates. $\underset{\sim}{K}$ indicates direction of wave propagation.

$$\underset{\sim}{u} = \underset{\sim}{f}(z)e^{i\left[\underset{\sim}{K}\ x-\omega t\right]} \tag{1}$$

As shown in Fig. 1, the wave propagation at an angle ϕ with the x-axis. Hence the wavenumber K is composed of x and y directional components which will be designated as k and ℓ, respectively. Thus $k = K\cos\phi$ and $\ell = K\sin\phi$, and

$$\underset{\sim}{u} = \underset{\sim}{f}(z)e^{i(kx+\ell y-\omega t)} \tag{2}$$

Using the method discussed in [13], $\underset{\sim}{u}$ is represented in terms of the pseudo-potentials, Θ, Φ, and ψ in the following form,

$$u_x = \frac{\partial\Theta}{\partial x},\ u_y = \frac{\partial\Phi}{\partial y} + \frac{\partial\Psi}{\partial z},\ u_z = \frac{\partial\Phi}{\partial z} - \frac{\partial\Psi}{\partial y}, \tag{3}$$

where,

$$\Theta = f_1(z)e^{i(kx+\ell y-\omega t)} \tag{4a}$$

$$\Phi = f_2(z)e^{i(kx+\ell y-\omega t)} \tag{4b}$$

$$\psi = f_3(z)e^{i(kx+\ell y-\omega t)} \tag{4c}$$

As seen in Fig. 1, the x-axis coincides with the axis of symmetry. The z-axis is in the direction of the thickness of the plate. The origin of the co-ordinates is

taken in the mid-plane of the plate, which is assumed to be of thickness, 2h. The y-axis is out of the plane of the diagram. Using the constitutive relation for the transversely isotropic materials considered in this paper, the equations of motion, and Eqs. (3-4) it can be shown that the functions f_1, f_2 and f_3 are given by

$$f_1(z) = F_1\Omega_1^+ + G_1\Omega_2^+$$

$$f_2(z) = F_2\Omega_1^+ + G_2\Omega_2^+ \tag{5}$$

$$f_3(z) = F_3\Omega_3^-$$

where

$$\Omega_1^+ = A_{11}\cos s_1 z + A_{12}\sin s_1 z$$

$$\Omega_2^+ = A_{21}\cos s_2 z + A_{22}\sin s_2 z \tag{6}$$

$$\Omega_3^- = A_{32}\cos rz - A_{31}\sin rz$$

The constants F_1, F_2, and G_1, G_2 can be chosen such that

$$\frac{F_1}{F_2} = -\delta(s^2_1+\ell^2)/(s^2_1+(\ell^2+\alpha k^2-K^2_2)) \tag{7a}$$

$$\frac{G_1}{G_2} = \frac{-\beta(s^2_2+\ell^2)-k^2+K^2_2}{\delta k_2} \tag{7b}$$

Note that s^2_1 and s^2_2 correspond to the + and - signs, respectively, in the expression for s^2 given below.

$$s^2 = \frac{\left\{[k_2^2(1+\beta)-k^2\gamma] \mp \sqrt{[K^2\gamma-K^2_2(1+\beta)]^2-4\beta(\alpha k^2-K^2_2)(k^2-K^2_2)}\right\}}{2\beta} - \ell^2. \tag{8}$$

Similarly, using Eq. (4c) and the expressions for $f_3(z)$ given above we get r to be

$$r = \left[\frac{[K^2_2-k^2-\ell^2\epsilon]}{\epsilon}\right]^{1/2} \tag{9}$$

We have define $\alpha = C_{11}/C_{55}$, $\beta = C_{33}/C_{55}$, $\gamma = C_{13}/C_{55}$, $\gamma = 1+\alpha\beta-\gamma^2$, $\epsilon = C_{44}/C_{55}$ and $K^2_2 = \rho\omega^2/C_{55}$.

With the expressions for Θ, Φ, and Ψ now completely determined, the traction components σ_{xz}, σ_{yz}, and σ_{zz} at the surface of the plate are set to zero. This leads to six linear homogeneous equations in the constants A_{11}, A_{12}, A_{31}, A_{12}, A_{22}, A_{33}. These equations can be grouped into a set of three equations with the first three

constants corresponding to the symmetric motion and another set containing the second three corresponding to the anti-symmetric motion. Note that the constants F_1, G_1, and F_3 may be taken as 1. and the other two constants F_2 and G_2 are then found from Eqs. (7a,b).

Thus, we obtain the dispersion equations for the symmetric and anti-symmetric modes of the plate as

$$\text{SYM:} \quad \left[\frac{E_{31}\Lambda_1}{E_{33}\Lambda_2} + \frac{\tan s_1 h}{\tan s_2 h}\right] \sin rh + \frac{E_{35}}{E_{33}\Lambda_2} \cos rh \tan s_1 h = 0 \tag{10a}$$

$$\text{ANTI-SYM;} \quad \left[\frac{E_{33}\Lambda_2}{E_{31}\Lambda_1} + \frac{\tan s_2 h}{\tan s_1 h}\right] \cos rh + \frac{E_{35}}{E_{31}\Lambda_1} \frac{\sin rh}{\tan s_2 h} = 0 \tag{10b}$$

$$\text{with } \Lambda_1 = \frac{E_{44}E_{66}-E_{64}E_{46}}{E_{42}E_{64}-E_{62}E_{44}} \text{ and } \Lambda_2 = \frac{E_{46}E_{62}-E_{42}E_{66}}{E_{42}E_{64}-E_{62}E_{44}},$$

where the expression for the E's are omitted here. These two equations are solved for the non-dimensional frequency, Ω, as a function of the wavenumber, ξ, which are defined as

$$\Omega = \frac{\omega H}{2\pi\sqrt{C_{55}/\rho}} \quad , \quad \xi = \frac{Kh}{2\pi} \, .$$

Once these roots are known the phase velocities are then calculated from the relation

$$C = \left[\frac{\Omega}{\xi}\right] \sqrt{C_{55}/\rho} \, .$$

In the following we present results for the non-dimensional phase velocity, $C/\sqrt{C_{55}/\rho}$, as a function of Ω.

DISCUSSION OF RESULTS

The two metal matrix materials were investigated to analyze the effects of anisotropy on the phase velocity diagram. The two materials and their constants are shown in Table 1. Gr/Mg material is a continuous fiber-reinforced composite, 60% by vol of graphite, while SiC/Al material is a particle-reinforced composite, 30% by vol of SiC in 6062 Al [1]. To show the degree of anisotropy of the materials velocity diagrams are shown in Figs. 2 and 3. In these figures the dash-dot lines represent the quasi-longitudinal wave, the dashed lines represent the quasi-shear wave, the solid lines represent the anti-plane shear waves and the three dot-dashed lines represent the Rayleigh wave velocity. As can be seen in Fig. 2, SiC/Al material shows small deviations from isotropy especially with the two shear surfaces crossing each other. Interesting is the Rayleigh velocity matching the quasi-shear velocity of propagation transverse to the fibers and the higher value of the anti-plane shear velocity as compared to the quasi-velocity. Moreover in Fig. 3, Gr/Mg material's large longitudinal wave velocity in the fiber direction is characteristic of substantial increase in the elastic stiffness in this direction over the other two directions. In all the velocity diagrams the ordinate represents the velocity at 90^0 and the abscissa represents the velocity at 0^0.

TABLE 1
All stiffnesses are in units of 10^{11} N/m^2

Materials	C_{11}	C_{33}	C_{13}	C_{44}	C_{55}
Gr/Mg	1.806	0.273	0.0956	0.0738	0.219
SiC/Al	1.419	1.729	0.677	0.513	0.429

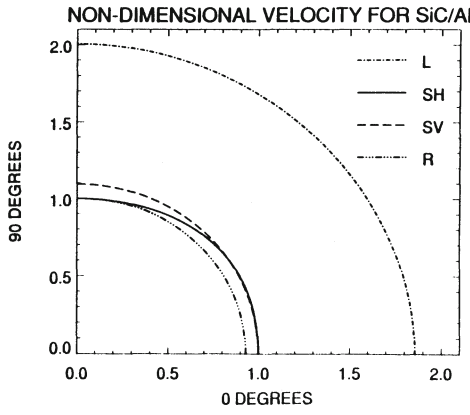

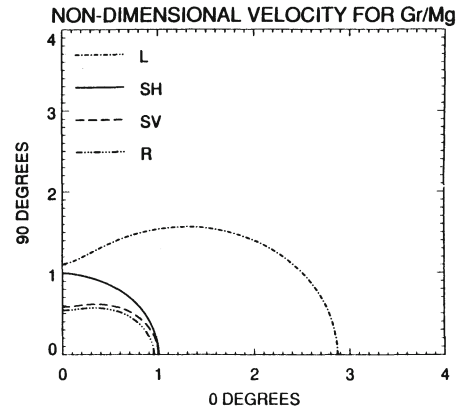

Figs. 2, 3. Velocity Diagrams for SiC/Al and Gr/Mg.

Consider now the phase velocity-frequency diagrams shown in Figs. 4 through 7. In Fig. 4 the normalized phase velocities for waves propagating parallel to the axis in the SiC/Al composite plate are shown for the symmetric branches. These graphs depict the dispersion behavior of guided waves in the plate. The dispersion Eqs. (10a) and (10b) do not give solutions for phase velocitites independent of frequencies, except for the first anti-plane shear wave propagating along the fiber and perpendicular to the fiber. The 0^{th} mode anti-plane shear velocity is unity in both Figs. 4 and 5 since it is normalized with respect to $\sqrt{C_{55}/\rho}$. Because of small anisotropy of the SiC/Al material, the dispersion characteristics in the plate are very similar to an isotropic one. The coupling of waves is not very strong. Thus, the curves for propagation at 45^0 to the x-axis are similar to those for 0^0 propagation. However, there are subtle differences as seen in Figs. 4 and 6. Of particular interest is to note that the symmetric in-plane and SH branches for 0^0 propagation cross, but that they come close without crossing for 45^0 propagation.

Figures 5 and 7 show the dispersion behavior in the Gr/Mg plate. The strong anisotropy of this material is seen to alter the dispersion characteristics drastically. It is found from Figs. 5 and 7 that the velocity curves for the symmetric modes show

two distinct plateaus: one at the longitudinal velocity in the plate and the other at the Rayleigh velocity (reached by the lowest modes) or the shear velocity (reached by the higher modes). The feature of (quasi) in-plane and (quasi) out-of-plane modes for off-axis propagation coming close to one another is strongly pronounced here also.

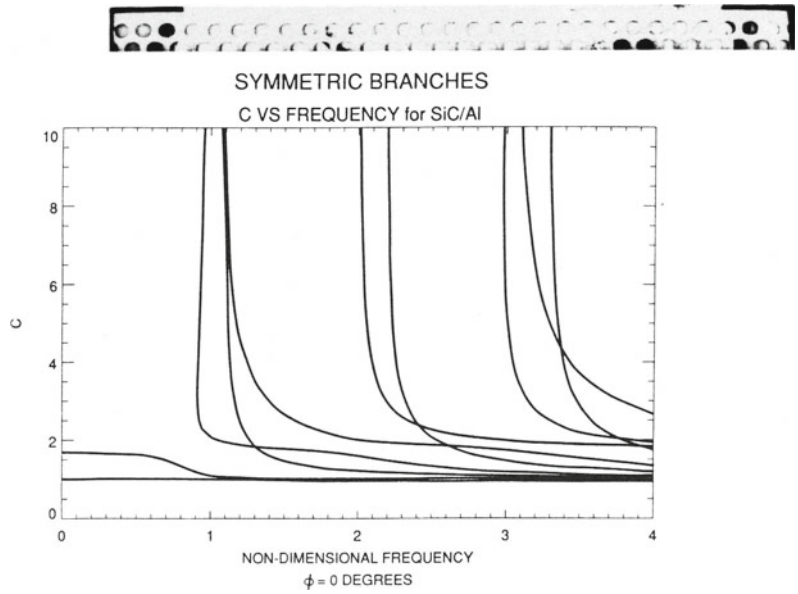

Fig. 4. Phase velocity for symmetric modes for propagation along the symmetry axis in the SiC/Al plate.

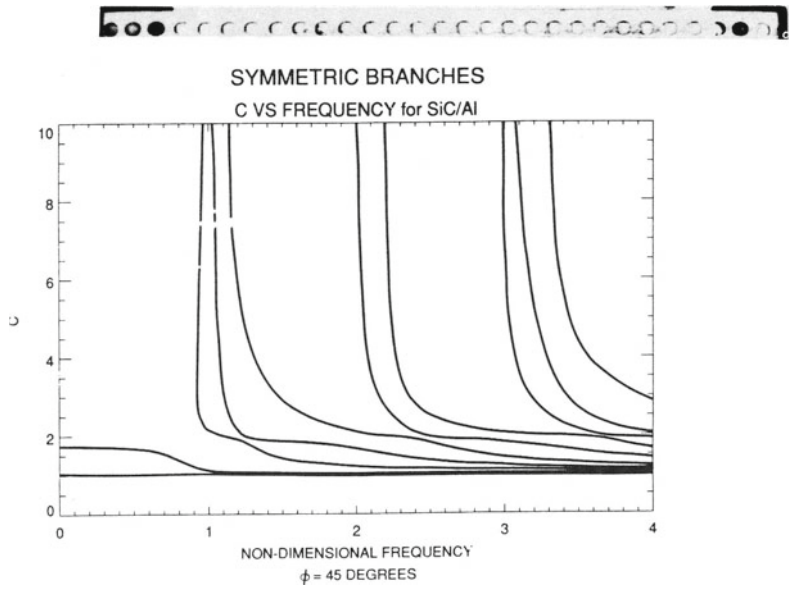

Fig. 5. Phase velocity for symmetric modes for propagation along the fiber direction in the Gr/Mg plate.

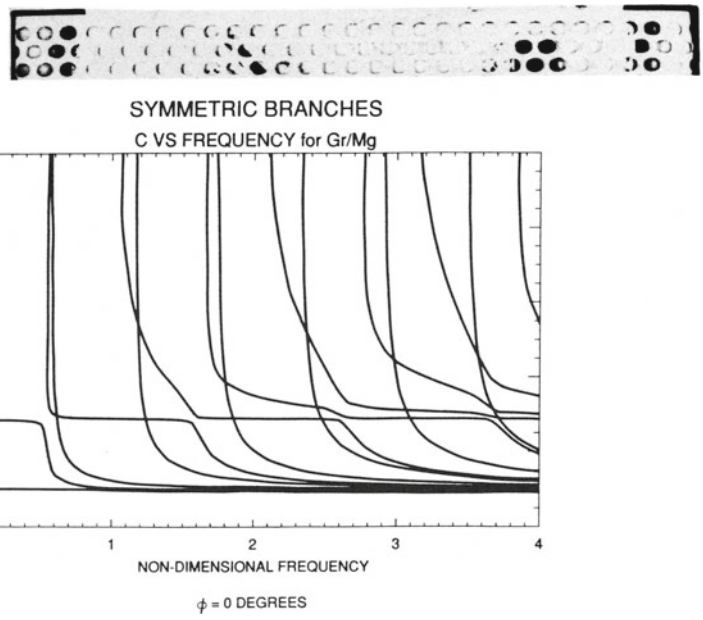

Fig. 6. Phase velocity for symmetric modes propagating at 45^0 to the symmetry axis in the SiC/Al plate.

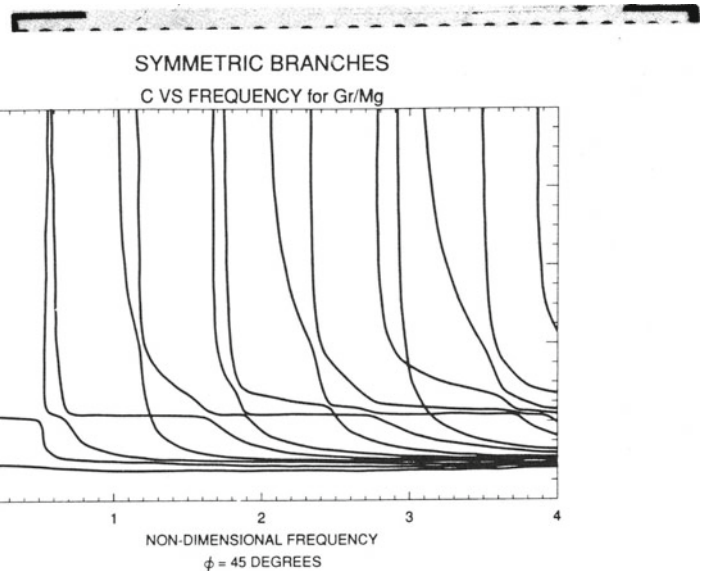

Fig. 7. Phase velocity for symmetric modes propagating at 45^0 to the fibers in the Gr/Mg plate.

CONCLUSION

In this paper we have shown the large differences that exist between the guided waves in two different anisotropic materials. Strong anisotropy in the longitudinal velocity in the Gr/Mg composite plate causes the phase velocities to drop rapidly with frequency to a plateau, which is the longitudinal velocity in the plate, and then to decrease to the Rayleigh velocity.

ACKNOWLEDGEMENT

The work reported here has been supported in part by a grant from the Office of Naval Research (00014-86-K-0280: Program Manager: Dr. Y. Rajapakse) and by grants from the National Science Foundation (MSDM-860913, INT-85214222, and INT-8610487). Support was received from the Natural Science and Engineering Research Council of Canada (A-7988).

REFERENCES

1. H. M. Ledbetter and S. K. Datta.J. Acoust. Soc. Am. 79, 239 (1986).
2. H. M. Ledbetter, S. K. Datta, and T. Kyono, submitted for publciation in the J. Appl. Phys. (1988).
3. R. D. Mindlin, Proceedings of the First Symposium on Naval Structural Mechanics (Pergamon Press, 1960), 199.
4. E. G. Newman and R. D. Mindlin, J. Acoust. Soc. Am. 34, (1962).
5. R. K. Kaul and R. D. Mindlin, J. Acoust. Soc. Am. 34, (1962).
6. R. D. Mindlin and M. A. Medick, J. Appl. Mech. 26, 561 (1959).
7. S. B. Dong and K. E. Pauley, J. Engr. Mech. Div. ASCE 104, 802 (1978).
8. S. B. Dong and K. H. Hwang, J. Appl. Mech. 52, 443 (1985).
9. S. K. Datta, A. H. Shaw, Y. Al-Nasser, and R. L. Bratton, Review of Progress in Quantitative Nondestructive Evaluation (Plenum Press, New York, 1988), 987.
10. S. K. Datta, A. H. Shah, R. L. Bratton, and T. Chakraborty, J. Acoust. Soc. Am. 83, 2020 (1988).
11. D. E. Chimenti and A. H. Nayfeh, J. Appl. Phys. 58, 4531 (1985).
12. A. H. Nayfeh and D. E. Chimenti, J. Acoust. Soc. Am. 83, 1736 (1988).
13. V. T. Buchwald, Quart. J. Mech. Appl. Math XIV, 293, (1961).